



**AFRL-HE-BR-TR-2007-0018**

**Experiments, Computation, and Modeling  
for Temperature Dependence of Absorption,  
Scattering, Reflection, Transmission, and Index of  
Refraction of Optical Radiation in Biological Tissues**

**Dhiraj K. Sardar  
Raylon M. Yow**

**University of Texas at Austin**

**Robert J. Thomas**

**Human Effectiveness Directorate  
Directed Energy Bioeffects Division  
Optical Radiation Branch**

**December 2006  
Final Report**

**DESTRUCTION NOTICE – Destroy by any method that will prevent disclosure  
of contents or reconstruction of this document.**

**Distribution Approved for Public Release;  
Distribution Unlimited**

**Air Force Research Laboratory  
Human Effectiveness Directorate  
Directed Energy Bioeffects Division  
Optical Radiation Branch  
Brooks City-Base, TX 78235**

## NOTICE AND SIGNATURE PAGE

Using Government drawings, specifications, or other data included in this document for any purpose other than Government procurement does not in any way obligate the U. S. Government. The fact that the Government formulated or supplied the drawings, specifications, or other data does not license the holder or any other person or corporation; or convey any rights or permission to manufacture, use, or sell any patented invention that may relate to them.

This report was cleared for public release by the Human Systems Wing (HSW/PA) Public Affairs Office and is available to the general public, including foreign nationals. Copies may be obtained from the Defense Technical Information Center (DTIC) (<http://www.dtic.mil>).

AFRL-HE-BR-TR-2007-0018 HAS BEEN REVIEWED AND IS APPROVED FOR PUBLICATION IN ACCORDANCE WITH ASSIGNED DISTRIBUTION STATEMENT.

//SIGNED//

ROBERT J. THOMAS, PhD  
Contract Monitor

//SIGNED//

GARRETT D. POLHAMUS, PhD, DR-IV  
Chief, Directed Energy Bioeffects Division

This report is published in the interest of scientific and technical information exchange, and its publication does not constitute the Government's approval or disapproval of its ideas or findings.

REPORT DOCUMENTATION PAGE			Form Approved OMB No. 0704-0188	
<p>Public reporting burden for this collection of information is estimated to average 1 hour per response, including the time for reviewing instructions, searching existing data sources, gathering and maintaining the data needed, and completing and reviewing this collection of information. Send comments regarding this burden estimate or any other aspect of this collection of information, including suggestions for reducing this burden to Department of Defense, Washington Headquarters Services, Directorate for Information Operations and Reports (0704-0188), 1215 Jefferson Davis Highway, Suite 1204, Arlington, VA 22202-4302. Respondents should be aware that notwithstanding any other provision of law, no person shall be subject to any penalty for failing to comply with a collection of information if it does not display a currently valid OMB control number. <b>PLEASE DO NOT RETURN YOUR FORM TO THE ABOVE ADDRESS.</b></p>				
1. REPORT DATE (DD-MM-YYYY) 12-11-2006	2. REPORT TYPE Final Technical Report	3. DATES COVERED (From - To) July 2005 – December 2006		
4. TITLE AND SUBTITLE  Experiments, Computation, and Modeling for Temperature Dependence of Absorption, Scattering, Reflection, Transmission, and Index of Refraction of Optical Radiation in Biological Tissues		5a. CONTRACT NUMBER FA8650-05-1-6641  5b. GRANT NUMBER  5c. PROGRAM ELEMENT NUMBER 62202F		
6. AUTHOR(S)  Sardar, Dhiraj K.; Yow, Raylon M.; Thomas, Robert J.		5d. PROJECT NUMBER 7757  5e. TASK NUMBER B2  5f. WORK UNIT NUMBER 30		
7. PERFORMING ORGANIZATION NAME(S) AND ADDRESS(ES)  Air Force Research Laboratory Human Effectiveness Directorate Directed Energy Bioeffects Division Optical Radiation Branch 2624 Louis Bauer Dr. Brooks City-Base, TX 78235-5128		8. PERFORMING ORGANIZATION REPORT NUMBER  AFRL/HEDO		
9. SPONSORING / MONITORING AGENCY NAME(S) AND ADDRESS(ES)  Air Force Materiel Command Air Force Research Laboratory Human Effectiveness Directorate Directed Energy Bioeffects Division Optical Radiation Branch 2624 Louis Bauer Dr. Brooks City-Base, TX 78235-5128		10. SPONSOR/MONITOR'S ACRONYM(S)  11. SPONSOR/MONITOR'S REPORT NUMBER(S) AFRL-HE-BR-TR-2007-0018		
12. DISTRIBUTION / AVAILABILITY STATEMENT DISTRIBUTION APPROVED FOR PUBLIC RELEASE; DISTRIBUTION UNLIMITED, PA 07-121, 12 APR 07.				
13. SUPPLEMENTARY NOTES Contract Monitor – Dr. Robert Thomas				
14. ABSTRACT <p>The objective of this research was to systematically measure the temperature dependence of optical properties of various bovine eye tissues at elevated temperatures (above body temperature) using different experimental and computational techniques. The temperature dependence of absorption and scattering coefficients of bovine ocular tissue in the temperature range of 24 to 40 degrees C at 980nm was measured. After computing diffuse reflectance and total transmittance, it was determined that any temperature dependence of the diffuse reflectance and total transmittance could not be discerned with the current setup in the temperature range of interest. The average diffuse reflectance and total transmittance values over all measured temperatures were input into the inverse adding doubling computer program. The resulting absorption coefficients were comparable to those reported by Sardar et al., but the scattering coefficients were not, perhaps due to some specular reflection inadvertently measured in the previous work. The rate of change of the refractive index with respect to temperature was performed at 632.8nm for bovine aqueous and vitreous humor in the temperature range of 37 to 41 degrees C. using the Mach-Zehnder interferometer setup. The measured refractive index with respect to temperature for bovine aqueous humor was comparable to that of water, while the measured value for bovine vitreous humor was slightly less than the value for water.</p> <p>These values are necessary for accurately modeling thermal lensing and hence light propagation in the eye.</p>				
15. SUBJECT TERMS: Laser, laser safety, directed energy bioeffects, optical properties review				
16. SECURITY CLASSIFICATION OF:		17. LIMITATION OF ABSTRACT	18. NUMBER OF PAGES	19a. NAME OF RESPONSIBLE PERSON Robert J. Thomas
a. REPORT Unclassified	b. ABSTRACT Unclassified	c. THIS PAGE Unclassified	SAR 24	19b. TELEPHONE NUMBER (include area code)

**This page intentionally left blank**

## TABLE OF CONTENTS

<b>List of Figures .....</b>	iv
<b>Summary .....</b>	1
<b>Temperature Dependence of Absorption and Scattering Coefficient .....</b>	1
Experimental Details .....	1
Inverse Adding Doubling (IAD) Method .....	3
Sample Preparation .....	4
Experimental Results .....	4
<b>Temperature Dependence of the Rate of Change of the Refractive Index with Respect to Temperature .....</b>	6
Experimental Details .....	6
Principle .....	8
Sample Preparation .....	9
System Calibration .....	9
Experimental Results .....	11
<b>Conclusion .....</b>	16
<b>References .....</b>	17
<b>Publications and Presentations .....</b>	18

## FIGURES

<b>Figure 1.</b> Setup for diffused reflectance and total transmittance measurements .....	2
<b>Figure 2.</b> Temperature controlled sample holder for diffused reflectance and total transmittance measurements .....	3
<b>Figure 3.</b> Diffuse reflectance ( $R_d$ ) data for bovine vitreous humor at 980nm. The dots are the average and the bars are the standard deviation of 10,000 data points .....	5
<b>Figure 4.</b> Total transmittance ( $T_t$ ) data for bovine vitreous humor at 980nm. The dots are the average and the bars are the standard deviation of 10,000 data points .....	5
<b>Figure 5.</b> Mach-Zehnder interferometer setup for measuring $\frac{\partial n}{\partial T}(T)$ .....	6
<b>Figure 6.</b> Temperature controlled sample holder for $\frac{\partial n}{\partial T}(T)$ measurements .....	7
<b>Figure 7.</b> Typical fringes observed with the setup in Fig. 5 .....	7
<b>Figure 8.</b> Refractive index values for water from Schiebener et al. <sup>3</sup> and best fit second and third order polynomials .....	10
<b>Figure 9.</b> Computed $\frac{\partial n}{\partial T}(T)$ curves for the best fit second and third order polynomials to Schiebener et al. <sup>3</sup> from 0 to 100C .....	10
<b>Figure 10.</b> Computed $\frac{\partial n}{\partial T}(T)$ curves for the best fit second and third order polynomials to Schiebener et al. <sup>3</sup> from 37 to 41C .....	11
<b>Figure 11.</b> Data and best fit for interference of water .....	12
<b>Figure 12.</b> Measured and best fit $\frac{\partial n}{\partial T}(T)$ for bovine aqueous humor at 632.8nm .....	13
<b>Figure 13.</b> Data and best fit for bovine aqueous humor at 632.8nm .....	13
<b>Figure 14.</b> Measured and corrected $\frac{\partial n}{\partial T}(T)$ for bovine aqueous humor at 632.8nm.....	14

**Figure 15.** Data and fit for bovine vitreous humor at 632.8nm.....14

**Figure 16.** Measured and corrected  $\frac{\partial n}{\partial T}(T)$  for bovine vitreous humor  
at 632.8nm .....15

**Figure 17.** Measured  $\frac{\partial n}{\partial T}(T)$  for water and bovine aqueous and  
vitreous humor at 632.8nm .....15

## **Experiments, Computation, and Modeling for Temperature Dependence of Absorption, Scattering, Reflection, Transmission, and Index of Refraction of Optical Radiation in Biological Tissues**

The objective of this research was to systematically measure the temperature dependence of optical properties of various bovine eye tissues using different experimental and computational techniques at elevated temperatures (above body temperature). An attempt was made to measure the temperature dependence of absorption and scattering coefficients of bovine ocular tissue in the temperature range of 24 to 40°C at 980 nm. The rate of change of the refractive index with respect to temperature was performed at 632.8 nm for bovine aqueous and vitreous humor in the temperature range of 37 to 41°C.

### **Temperature Dependence of Absorption and Scattering Coefficient**

#### **Experimental Details**

The schematic of the experimental setup for measuring the temperature dependent total diffuse reflectance and total transmittance of bovine ocular tissue is shown in Fig.1. Two identical integrating spheres (Newport 70674) each of diameter 150 mm with port apertures of 11 mm in diameter were utilized. A laser beam was split by a 30-70 beam splitter (BS) which directed 30 percent of the light to the reference sphere and the remaining 70 percent of the light toward entrance port I of the sample sphere. The tissue under study was placed in a temperature-controlled sample holder whose details are shown in Fig. 2. The sample holder was made from 6.44 mm thick aluminum and had two 1 mm thick glass windows. The aperture of the sample chamber was approximately 16 mm in diameter. The sample holder had two heaters (Omega SRFG101) attached to one side. The temperature of the sample was elevated by controlling the voltage across the heating elements with a variable voltage supply (Powerstat 3PN116B) and measuring the temperature with a digital thermometer (Hart Scientific 1006). For total transmission measurements, the sample holder was mounted to port I of the sample sphere while a port II of the sample sphere was covered with a cap with a reflective surface identical to that of the integrating spheres. For total diffused reflectance measurements, the sample holder was mounted to port II of the sample sphere while a port I was open. The sample holder was thermally insulated from the sample sphere by a 1 mm thick polycarbonate spacer.

The measurements were performed on bovine vitreous humor at 980 nm in the temperature range of 21 – 40°C. The 980 nm wavelength was supplied by pig-tailed diode lasers (Thorlabs model L9805E2P5) coupled to a collimator (Thorlabs model F220FC-C) and controlled by a Thorlabs (model LDC 2000) laser driver. The laser beam diameter at  $1/e^2$  of the peak intensity was 1.97 mm and beam divergence was about 0.048°. The average output power was kept at about 0.25 mW for all optical measurements.

The reflected and transmitted light intensities were detected by two identical infrared detectors (Judson J16-D) attached to the two measuring ports of the integrating spheres. The detector signal was sent to identical preamplifiers (Judson PA-9) powered by a common power supply (Pasco 8000). Signals from the detectors were measured and recorded by a digital oscilloscope (Tektronix TDS3054B). The measured light intensities were then utilized to determine the total diffuse reflectance  $R_d$  and total transmittance  $T_t$  by the following expressions:

$$R_d = \frac{X_R - C_{XR}}{2.33(Z_R - C_{ZR})} \quad (1)$$

and

$$T_t = \frac{X_T - C_{XT}}{2.33(Z_T - C_{ZT})} \quad (2)$$

where  $X_R$  is the measurement at the sample sphere with the sample at port II,  $Z_R$  is the measurement at the reference sphere,  $C_{XR}$  is the correction factor for stray light measured at the sample sphere with no sample at port I and port II uncovered and the laser on, while  $C_{ZR}$  is the correction for the reference sphere with the laser off. For the total transmittance measurements,  $X_T$  is the measurement at the sample sphere with the sample at port I,  $Z_T$  is the measurement at the reference sphere,  $C_{XT}$  is the correction factor for the sample sphere measured with no sample at port I, port II covered and the laser off, while  $C_{ZT}$  is the correction for the light in the reference sphere with the laser off. The 2.33 term is 70/30 to account for the beam splitter difference.

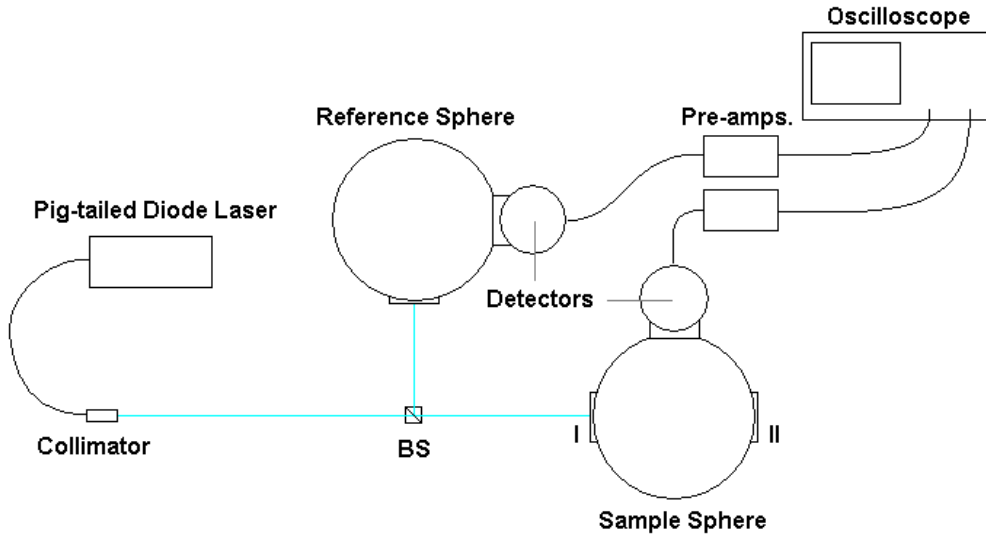


**Fig. 1.** Setup for diffused reflectance and total transmittance measurements.

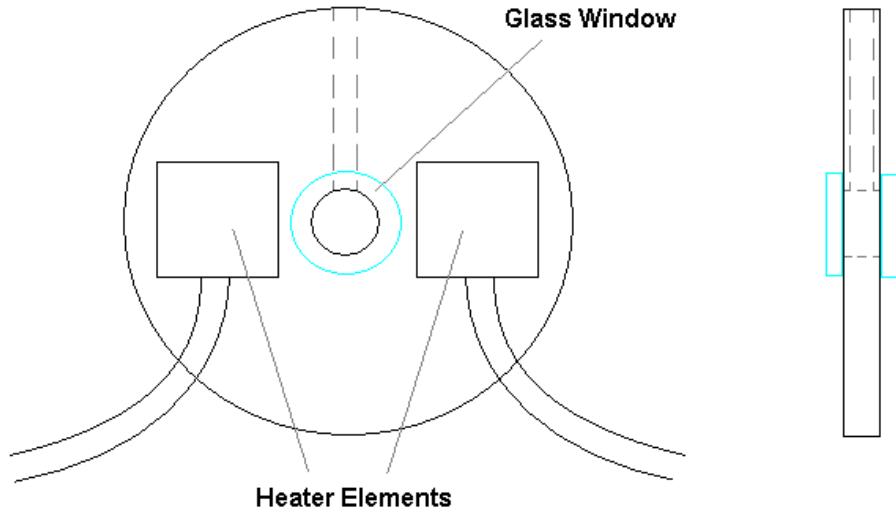


**Fig. 2.** Temperature controlled sample holder for diffused reflectance and total

### Inverse Adding Doubling (IAD) Method

The IAD computer program was used to solve the radiative transport equation. The IAD computer program must be supplied with the experimental values of total diffuse reflectance ( $R_d$ ) and total transmittance ( $T_t$ ) along with values of index of refraction ( $n$ ) and scattering anisotropy ( $g$ ) of the sample. The IAD program guesses a set of optical properties ( $a$  and  $\tau$ , defined below) and then calculates values for  $R_d$  and  $T_t$ . This process is repeated until the calculated and measured values of  $R_d$  and  $T_t$  are within a specified tolerance. Values of  $a$  and  $\tau$  provided by the IAD method are used to calculate the absorption coefficient ( $\mu_a$ ) and scattering coefficient ( $\mu_s$ ) for individual tissue using Eqs. (3) and (4).

$$a = \mu_s / (\mu_s + \mu_a) \quad (3)$$

$$\tau = t (\mu_s + \mu_a), \quad (4)$$

In the above  $t$  is the physical thickness of the sample measured in cm.

According to Prahl et al.<sup>1</sup>, the validity of the IAD method for samples with comparable absorption and scattering coefficients is especially important, since other methods based on only diffusion approximation are inadequate. They have also stated that since both anisotropy phase function and Fresnel reflection at boundaries is accurately approximated, the IAD method is well suited to optical measurements for biological materials sandwiched between two glass slides. Details of the IAD method have been previously provided by Prahl et al.

## Sample Preparation

One pair of bovine eyes was procured from a local slaughterhouse. This pair of eyes was enucleated fresh, packed on ice and immediately transported to the research laboratory (within one hour). Immediately upon arrival at the research laboratory, fresh (not frozen) whole eyes were dissected on ice to remove vitreous humor for optical measurements. Approximately three milliliters of vitreous humor was removed from the bisected bovine eye using a 1cc tuberculin syringe, sans the fine needle. Vitreous humor was then introduced into the sample holder described above and shown in Fig. 2. Visual inspection showed clear vitreous humor at the time when optical measurements were conducted.

## Experimental Results

The diffuse reflectance ( $R_d$ ) and total transmittance ( $T_t$ ) of the bovine vitreous humor at 980 in the temperature range of 24 to 40°C are given in Figs. 3 and 4, respectively. There seemed to be little correlation between  $R_d$  or  $T_t$  and temperature. A repeat of the total transmittance measurements at 23°C at five-minute intervals, roughly the same duration between temperature readings, for ten readings is shown in Fig. 4. Note the spread of the data at this one temperature is close to that of the data taken at other temperatures. It was thus concluded that any temperature dependence of the diffuse reflectance and total transmittance could not be discerned with the current setup. No attempt was made at any other wavelengths for any sample.

The absorption and scattering coefficient for the bovine vitreous humor from the data averaged over all temperatures was determined to be  $0.75 \text{ cm}^{-1}$  and  $0.03 \text{ cm}^{-1}$ , respectively. The refractive index and anisotropy were considered to be independent of temperature and taken from Sardar et al.<sup>2</sup> to be 1.33 and 0.99, respectively. Values for absorption and scattering coefficient for bovine vitreous humor at room temperature reported by Sardar et al. are  $1.27 \text{ cm}^{-1}$  and  $0.88 \text{ cm}^{-1}$ , respectively. Though the absorption coefficients are comparable the scattering coefficients are not. It is possible that some specular reflection was inadvertently measured in the work done by Sardar et al.

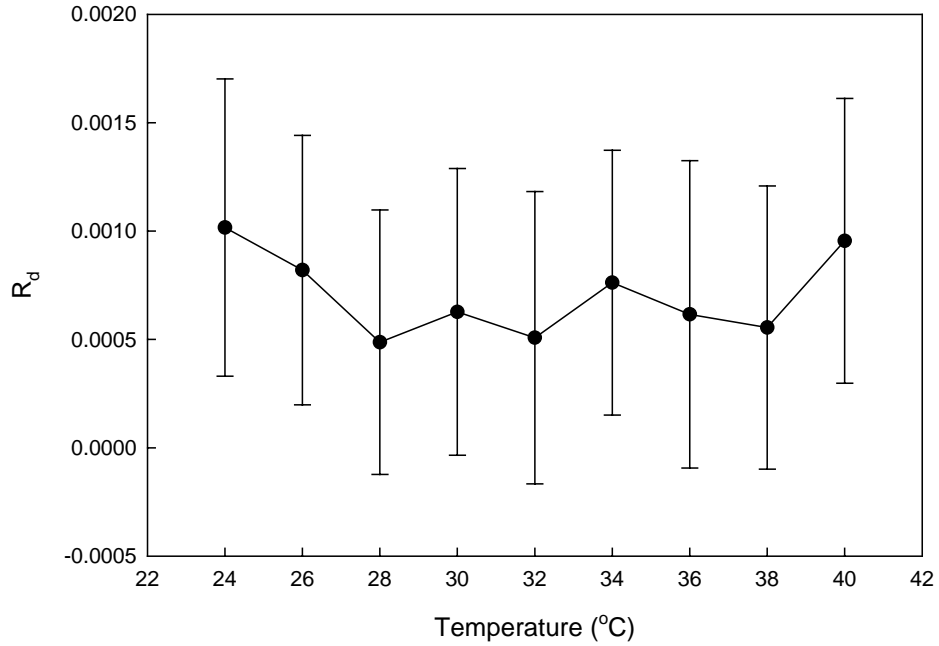


**Fig. 3.** Diffuse reflectance ( $R_d$ ) data for bovine vitreous humor at 980nm. The dots are the average and the bars are the standard deviation of 10,000 data points.

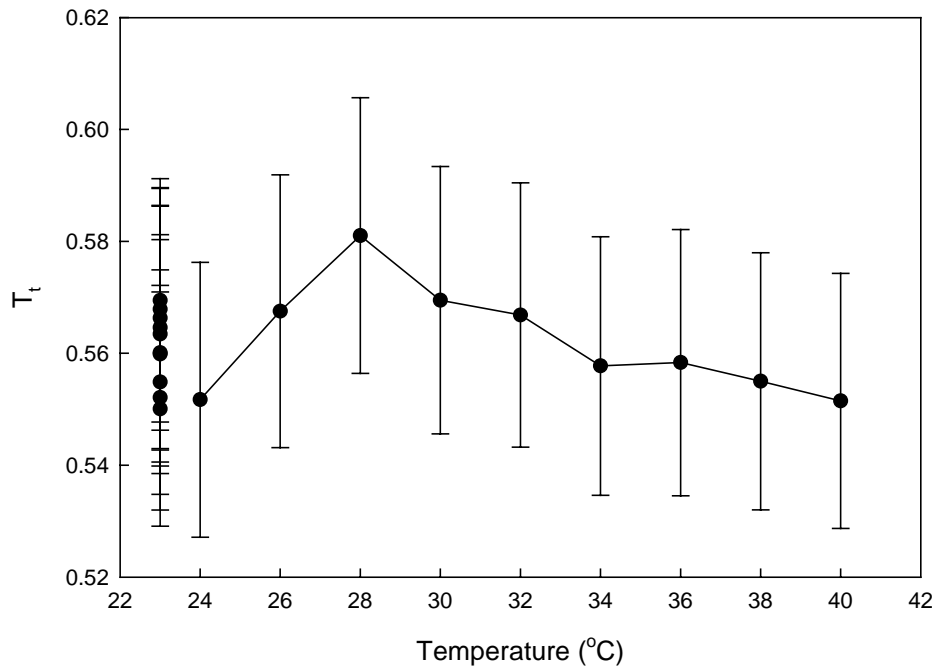


**Fig. 4.** Total transmittance ( $T_t$ ) data for bovine vitreous humor at 980nm. The dots are the average and the bars are the standard deviation of 10,000 data points.

## Temperature Dependence of $\frac{\partial n}{\partial T}$

### Experimental Details

In the current work, we use a Mach-Zehnder interferometer to measure the  $\frac{\partial n}{\partial T}(T)$  parameter without knowing the actual value of the refractive index. The schematic of which is shown in Fig. 5 where BS1 and BS2 are beam splitters and M1 and M2 are mirrors. The paths BS1-M1-BS2 and BS1-M2-BS2 are referred to as the reference arm and the sample arm of the interferometer, respectively.

The tissue was placed in the sample arm of the interferometer using a temperature-controlled sample holder, the details of which are shown in Fig. 6. The sample holder was constructed from aluminum 9.67 mm thick with an aperture of about 12 mm in diameter and had two 1 mm thick glass windows. Two electric heating elements (Omega SRFG101) were affixed to either side of the sample holder. The current through the heater, and thus the heat introduced into the system, was controlled by a voltage regulator (Powerstat 3PN116B). The temperature of the sample was monitored by an electronic thermometer system (Hart Scientific 1006). In the current study data was recorded from 37 to 41°C at 0.05°C intervals. The interferograms were captured by a CCD camera (Spiricon Cohu 4800) and recorded as bitmap images for final analysis. A typical fringe interferogram for the setup used here is shown Fig. 7. The light source of the interferometer was a 5 mW helium-neon laser (Electro-Optics LHRP-0501) at wavelength 632.8 nm.

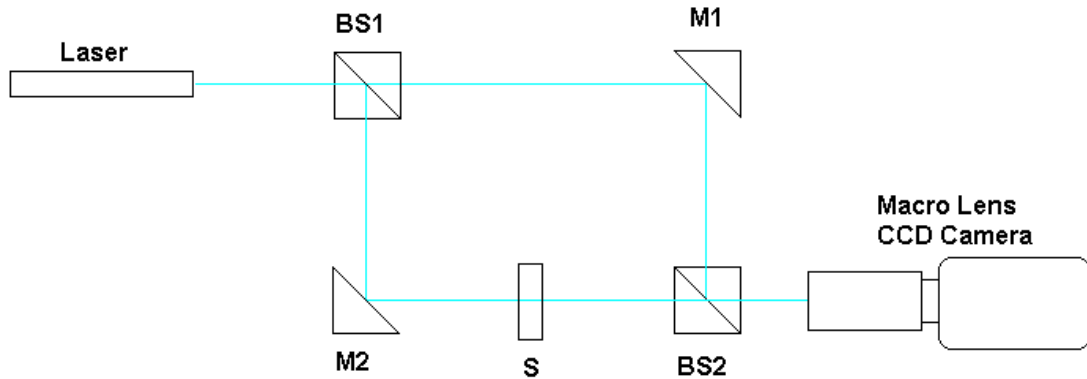


**Fig. 5.** Mach-Zehnder interferometer setup for measuring  $\frac{\partial n}{\partial T}(T)$ .

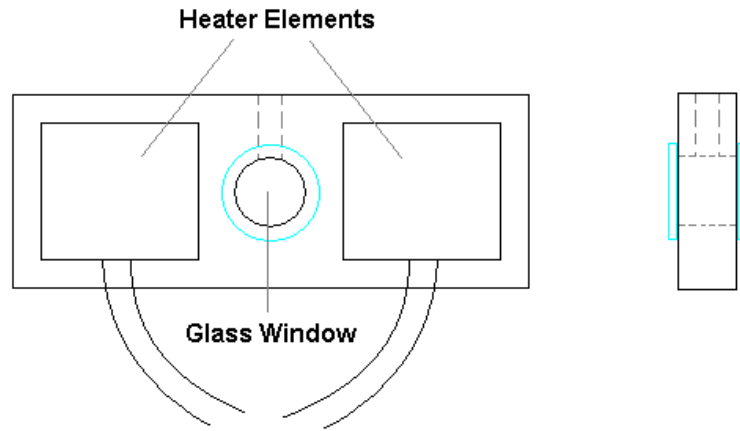


**Fig. 6.** Temperature controlled sample holder for  $\frac{\partial n}{\partial T}(T)$  measurements.

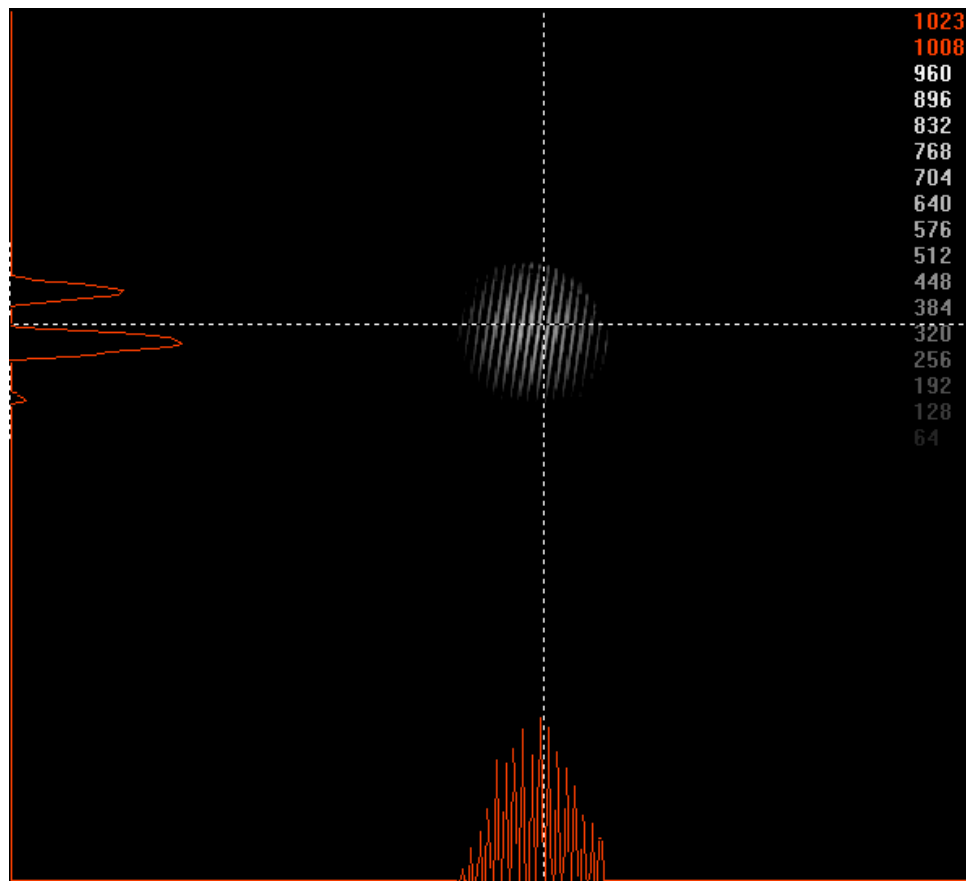


**Fig. 7.** Typical fringes observed with the setup in Fig. 5.

## Principle

For our experimental conditions, the thickness of the sample in the optical pathway was 9.67 mm, and we assumed that the sample difference in the direction of the optical pathway is negligible. In such case we can treat the problem two dimensionally so that every point in the observed region can be expressed by an orthogonal coordinate  $(x,y)$ . If we study the sample only, and suppose that the initial refractive index of the solution is  $n(x, y, T_0)$ , after a small change in temperature  $\Delta T$  the refractive index changes to  $n(x, y, T_0 + \Delta T)$  at the point  $(x,y)$ . The phase change at point  $(x,y)$  is thus  $\phi(x, y, T_0 + \Delta T) - \phi(x, y, T_0)$ , and we have:

$$[n(x, y, T_0 + \Delta T) - n(x, y, T_0)]d = \frac{\lambda}{2\pi} [\phi(x, y, T_0 + \Delta T) - \phi(x, y, T_0)] \quad (5)$$

Dividing both sides of equation 5 by the thickness,  $d$ , and  $\Delta T$  and taking the limit as  $\Delta T$  tends to 0, we get:

$$\frac{\partial n}{\partial T}(x, y, T) = \frac{\lambda}{2\pi d} \frac{\partial \phi}{\partial T}(x, y, T) \quad (6)$$

Fixing the point  $(x,y)$  we get:

$$\frac{\partial n_{x,y}}{\partial T}(T) = \frac{\lambda}{2\pi d} \frac{\partial \phi_{x,y}}{\partial T}(T) \quad (7)$$

Hence, once  $\frac{\partial \phi}{\partial T}(T)$  is known,  $\frac{\partial n}{\partial T}(T)$  can be determined. We determine the term  $\frac{\partial \phi}{\partial T}(T)$  from an interferometric setup as discussed below.

For a 50-50 interferometer, the interference term for the intensity,  $I_{\text{int}}$ , is given by:

$$I_{\text{int}} = 2I \cos(\delta\phi) \quad (8)$$

where  $I$  is the laser intensity and  $\delta\phi$  is the phase difference between the two paths. For wide field, temperature dependent, equation 8 takes the form:

$$I_{\text{int}}(x, y, T) = 2I \cos(\delta\phi(x, y, T)) \quad (9)$$

Fixing the point  $(x,y)$  we can expand the phase difference as:

$$\delta\phi_{x,y}(T) = a'_0 + a_1 T + a_2 T^2 + a_3 T^3 \quad (10)$$

Since the reference arm of the interferometer is at a fixed temperature, we can absorb the difference in phase at the initial temperature into the constant  $a'_0$  to get another constant  $a_0$ , and thus we can recast equation 10 as:

$$\phi_{x,y}(T) = a_0 + a_1 T + a_2 T^2 + a_3 T^3 \quad (11)$$

where  $\phi_{x,y}(T)$  is now the phase of the light passing through the sample relative to the reference path as a function of sample temperature.

Thus for a given point (x,y) we have the model:

$$I_{\text{int } x,y}(T) = \max(0, A \cos(a_0 + a_1 T + a_2 T^2 + a_3 T^3) + B) \quad (12)$$

where the  $B$  term is needed to account for the threshold to be overcome in the detector and the max term is needed since the intensity cannot be less than zero. It is this model that we fit observed data from a Mach-Zehnder interferometer to obtain  $\phi(T)$  which is then differentiated to obtain  $\frac{\partial \phi}{\partial T}(T)$  then scaled by  $\frac{\lambda}{2\pi d}$  (equation 7) to obtain  $\frac{\partial n}{\partial T}(T)$ .

### Sample Preparation

Two pairs of bovine eyes were procured from a local slaughterhouse. These pairs of eyes were enucleated fresh, packed on ice and immediately transported to the research laboratory (within one hour). Immediately upon arrival at the research laboratory, fresh (not frozen) whole eyes were dissected on ice to remove aqueous vitreous humor for optical measurements. Approximately three milliliters of aqueous humor was removed from the two bisected bovine eye using a 1cc tuberculin syringe. Aqueous humor was then introduced into the sample holder described above and shown in Fig. 6. For the vitreous humor, approximately three milliliters of vitreous humor was removed from a bisected bovine eye using a 1cc tuberculin syringe, sans the fine needle. Vitreous humor was then introduced into the sample holder after the experiment was performed for the aqueous humor and the sample holder washed. Visual inspection showed clear aqueous and vitreous humor at the time when optical measurements were conducted.

### System Calibration

As a means of calibrating our setup, we relied on the data of Schiebener et al.<sup>3</sup> To obtain a closed form solution of the refractive index of water at 632.8 nm at atmospheric pressure we best fit the data reported by Schiebener et al. to polynomials of second and third order. Both polynomials give a good fit to the refractive index data for water reported in Schiebener et al. as shown in Fig. 8. Differentiating the best-fit polynomials however reveals considerable difference between the second and third order polynomials as shown in Fig. 9. Significant difference between the two occurs in our temperature range of interest of 37 to 41°C (see Fig. 10). We hence use a third order polynomial as the true fit for the data reported in Schiebener et al.

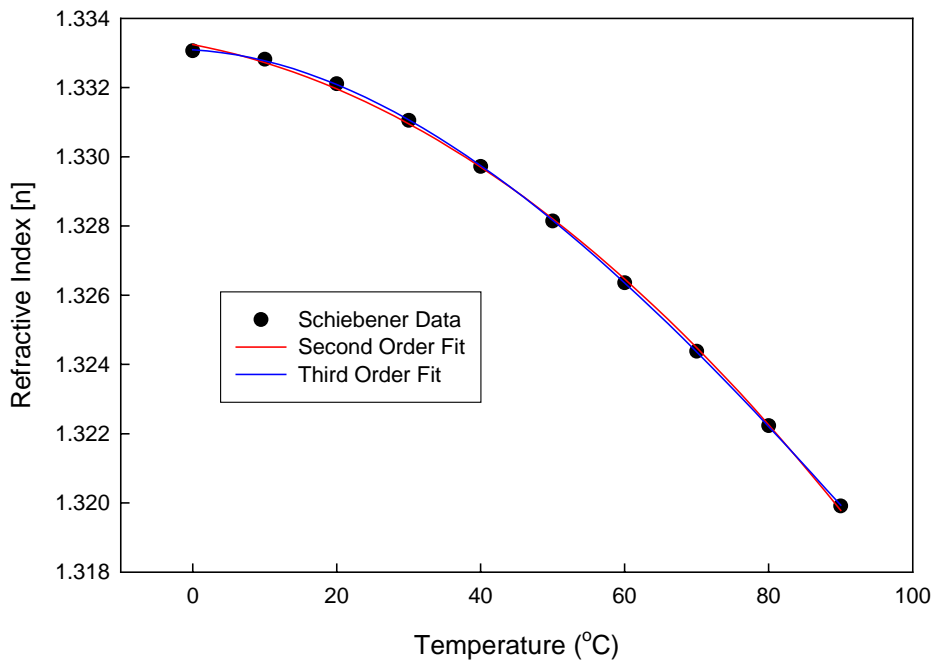


**Fig. 8.** Refractive index values for water from Schiebener et al.<sup>3</sup> and best fit second and third order polynomials.

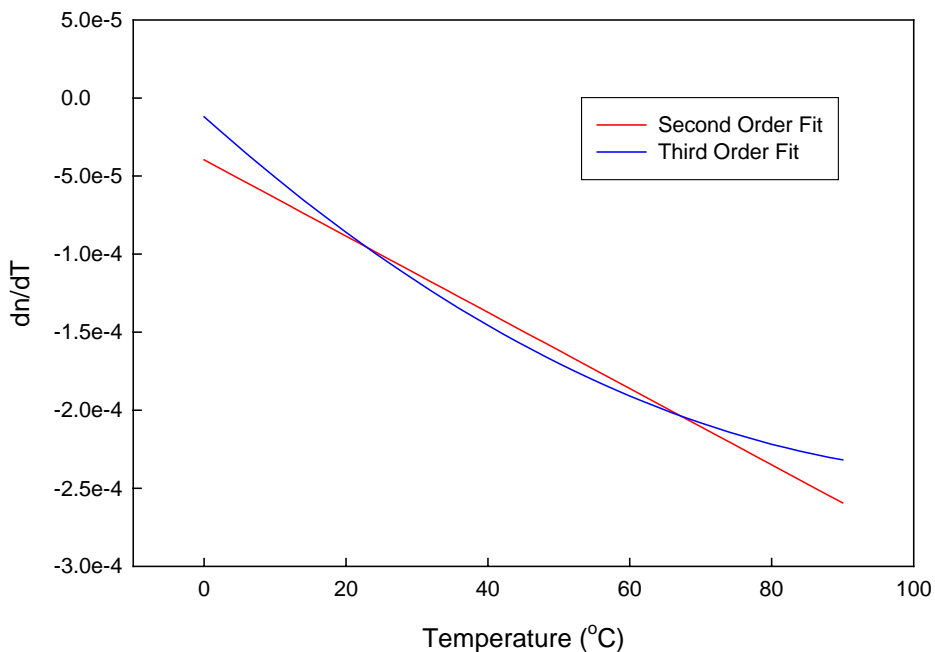


**Fig. 9.** Computed  $\frac{\partial n}{\partial T}(T)$  curves for the best fit second and third order polynomials to Schiebener et al.<sup>3</sup> from 0 to 100°C.

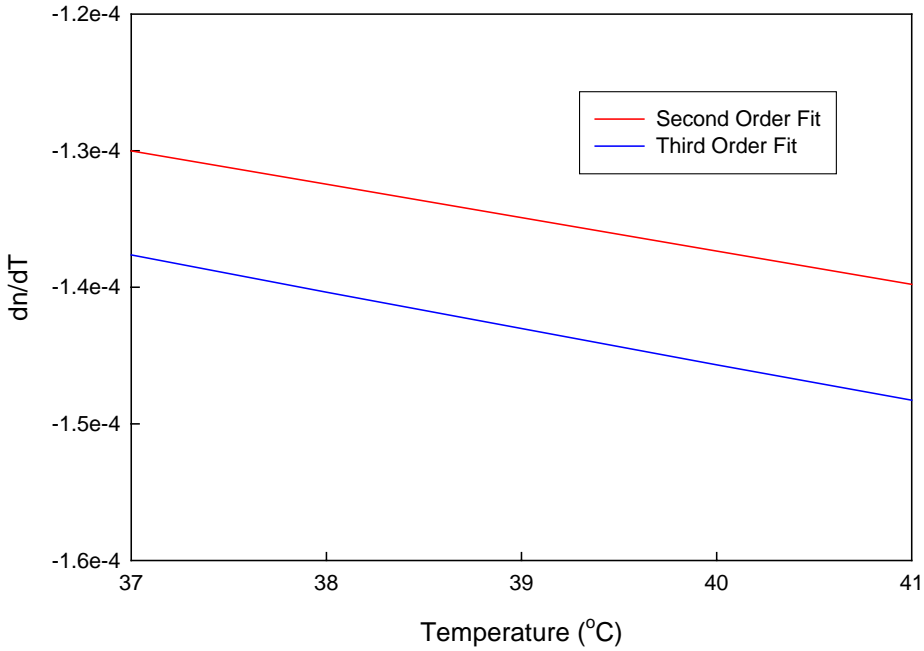


**Fig. 10.** Computed  $\frac{\partial n}{\partial T}(T)$  curves for the best fit second and third order polynomials to Schiebener et al.<sup>3</sup> from 37 to 41°C.

## Experimental Results

For all experiments the voltage across the four resistive heaters was set to 30.0 volts resulting in a temperature increase rate of about 0.005°C/second throughout the temperature range of 37 to 41°C. The intensity captured by the CCD camera for water for a given pixel is shown in Fig. 11 as solid dots. The best fit to this curve, obtained by a genetic algorithm written in Matlab, for equation 13 is shown as the solid line. The difference in the calculated and the fitted data from Schiebener et al.<sup>3</sup> is shown as the green line in Fig. 12. This is taken as the correction factor for our experimental setup, which is thought to be due to the phase shift induced by the glass windows on either side of the sample. A comparison to literature<sup>4</sup> gives  $\frac{\partial n}{\partial T}(T)$  for glass to be of the order of magnitude of  $10^{-5}$ , comparable to our results. The same experiment for bovine aqueous humor and vitreous humor at 632.8 nm were performed. Figs. 13 and 15 show the experimental values and best fit for the intensity as a function of temperature for bovine aqueous humor and vitreous humor, respectively. Figs. 14 and 16 show the calculated  $\frac{\partial n}{\partial T}(T)$  for the measured samples plus the corrected values for bovine aqueous humor and vitreous humor, respectively.

For bovine aqueous humor the best fit to measured data yielded:

$$\frac{\partial n}{\partial T}(T) = 8.268 \times 10^{-4} - 4.313 \times 10^{-5} T + 4.960 \times 10^{-7} T^2 \quad (13)$$

For bovine vitreous humor the best fit to measured data yielded:

$$\frac{\partial n}{\partial T}(T) = 5.815 \times 10^{-3} - 3.000 \times 10^{-4} T + 3.758 \times 10^{-6} T^2 \quad (14)$$

These values are of the same order of magnitude of water as shown in Fig. 17. Note that  $\frac{\partial n}{\partial T}(T)$  for bovine aqueous humor is close to that of water. Depending on the precision required for the value of  $\frac{\partial n}{\partial T}(T)$  it may suffice to take  $\frac{\partial n}{\partial T}(T)$  for bovine aqueous humor to be that of water.

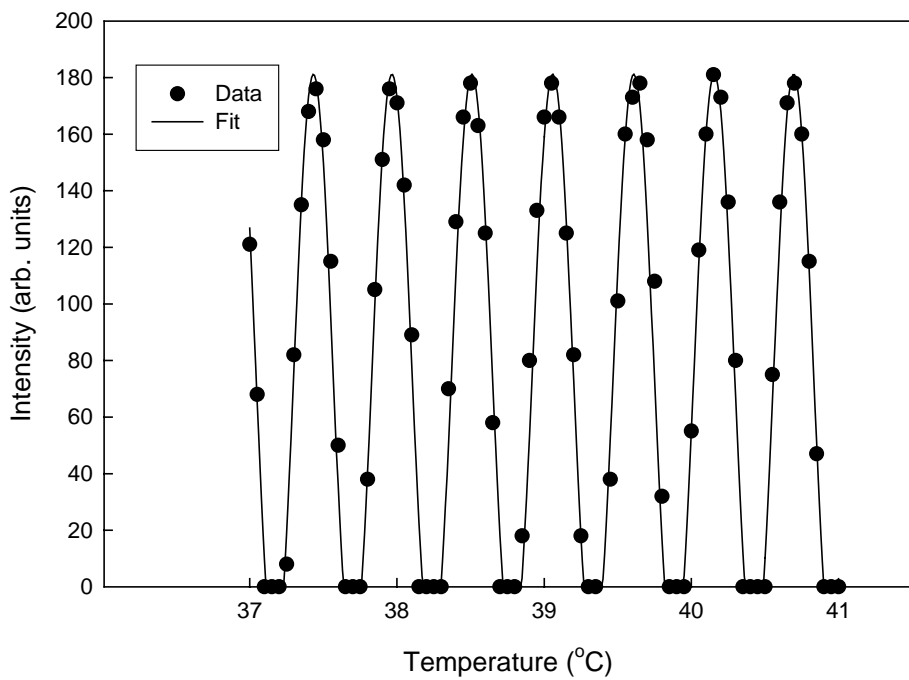


**Fig. 11.** Data and best fit for interference of water.

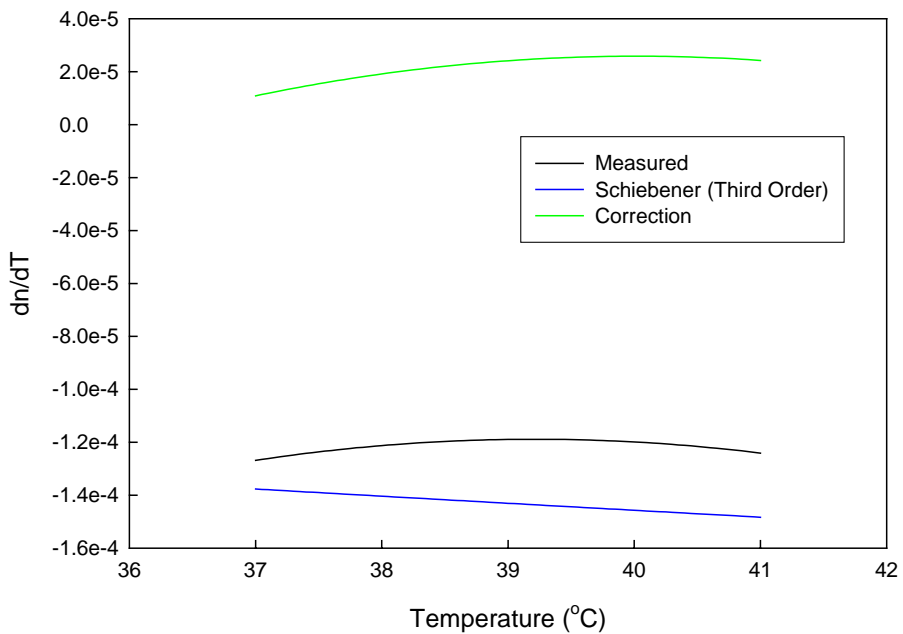


**Fig. 12.** Measured and best fit  $\frac{\partial n}{\partial T}(T)$  for water along with the correction at 632.8 nm.

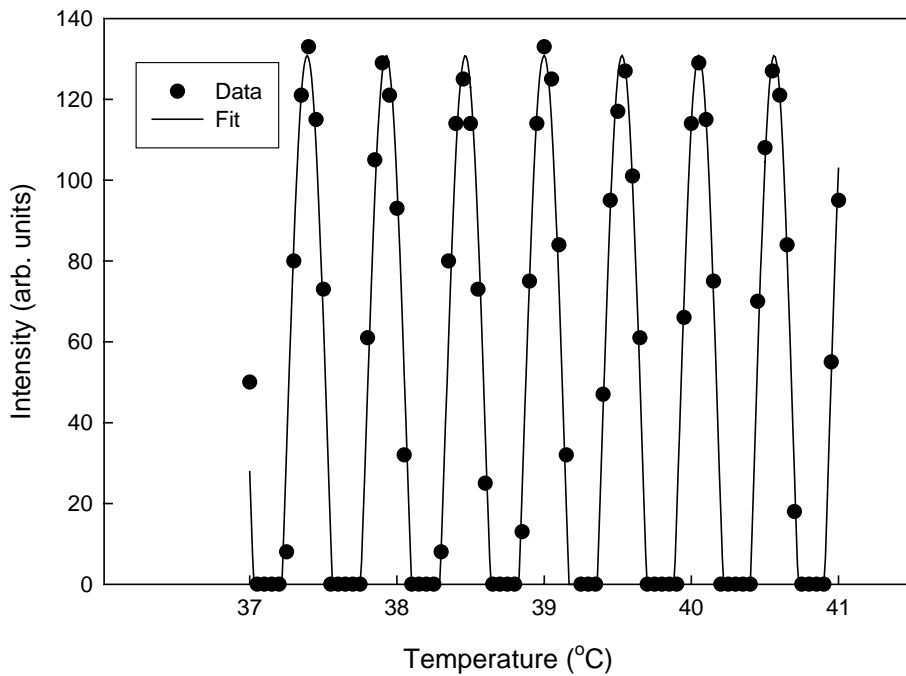


**Fig. 13.** Data and fit for bovine aqueous humor at 632.8 nm.

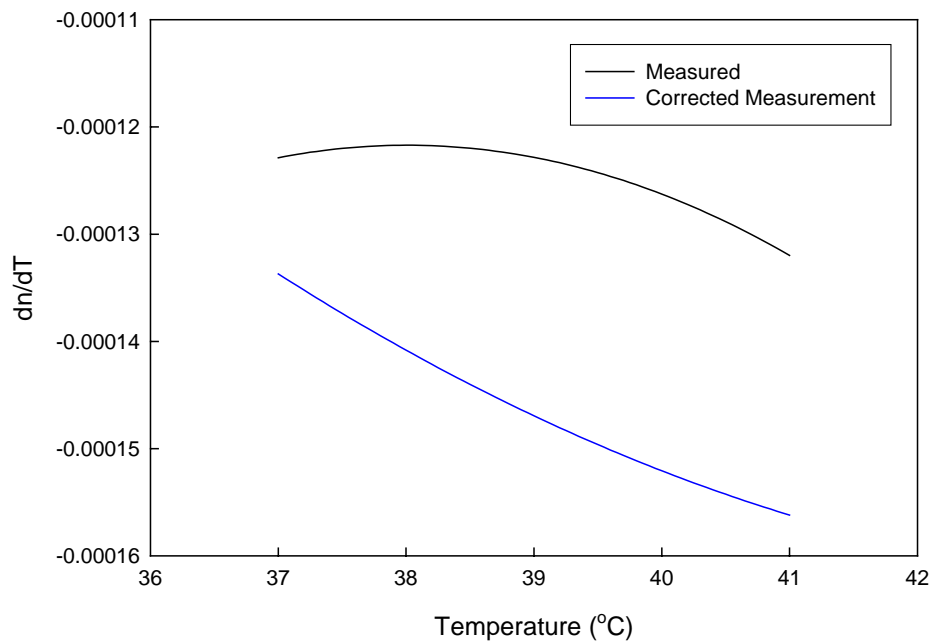


**Fig. 14.** Measured and corrected  $\frac{\partial n}{\partial T}(T)$  for bovine aqueous humor at 632.8 nm.

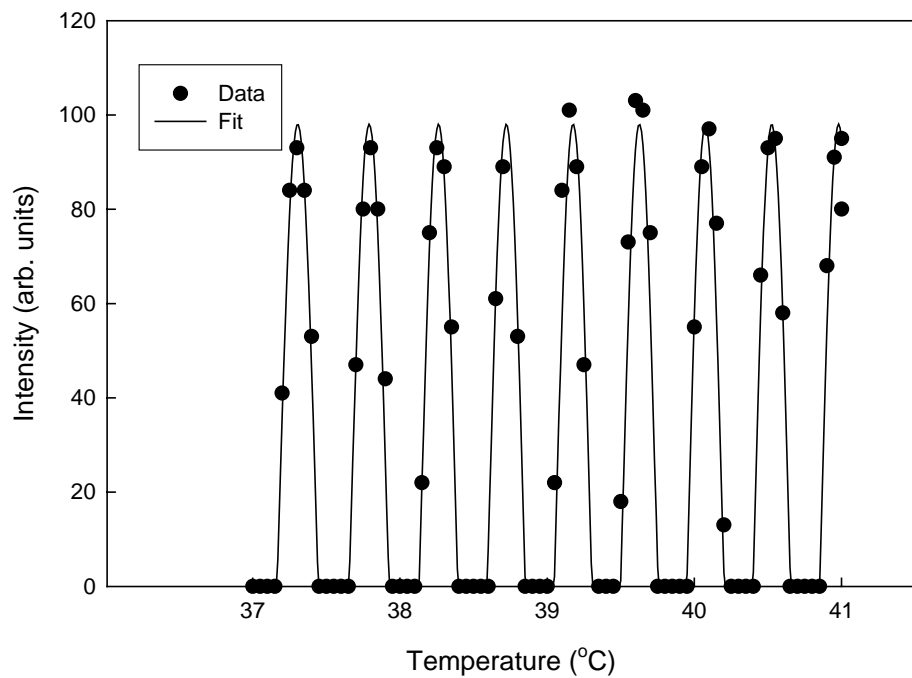


**Fig. 15.** Data and fit for bovine vitreous humor at 632.8 nm.

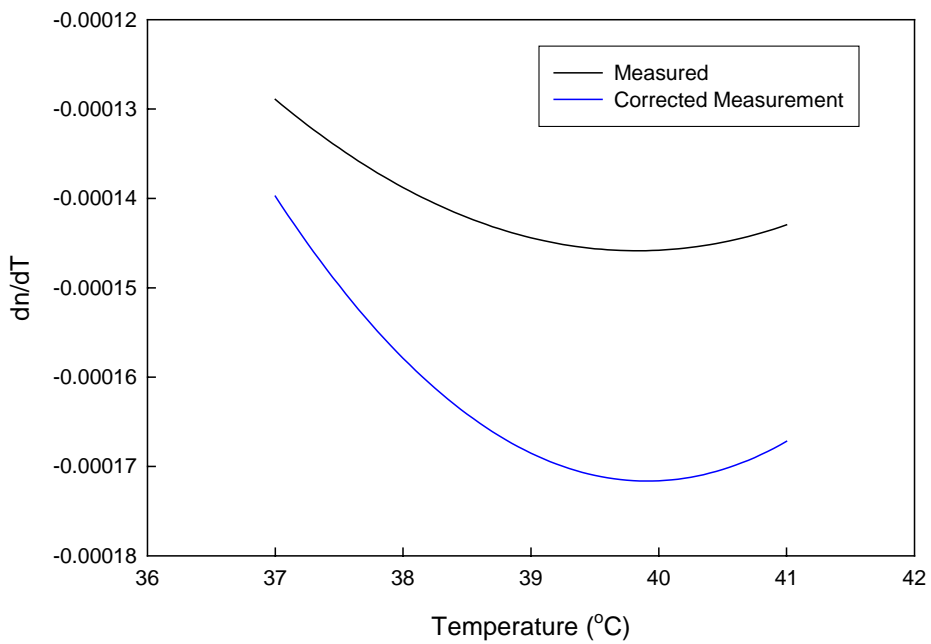


**Fig. 16.** Measured and corrected  $\frac{\partial n}{\partial T}(T)$  for bovine vitreous humor at 632.8 nm.

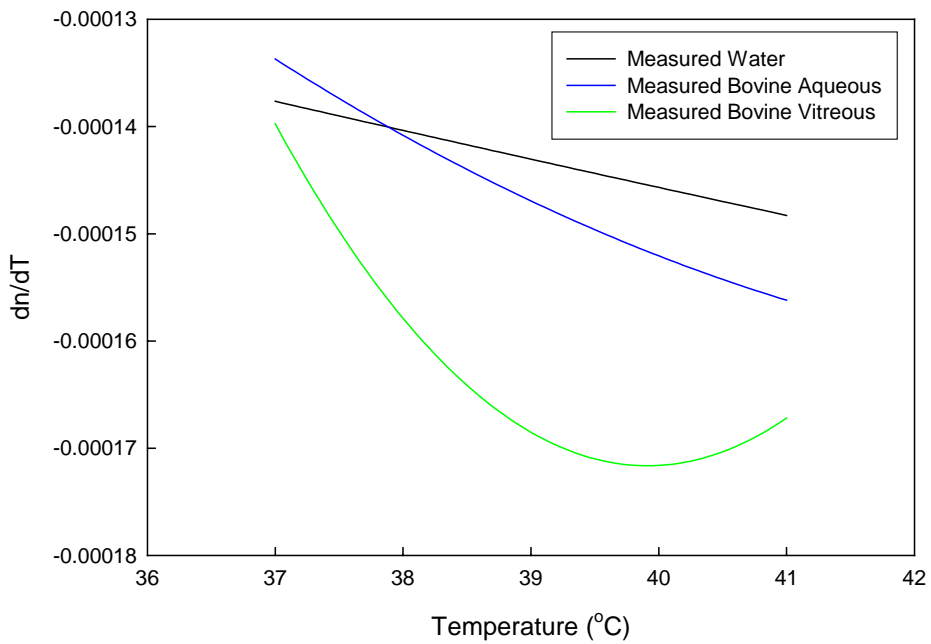


**Fig. 17.** Measured  $\frac{\partial n}{\partial T}(T)$  for water and bovine aqueous and vitreous humor at 632.8 nm.

## Conclusion

The objective of this research was to systematically measure the temperature dependence of optical properties of various bovine eye tissues using different experimental and computational techniques at elevated temperatures (above body temperature).

The diffuse reflectance ( $R_d$ ) and total transmittance ( $T_t$ ) of the bovine vitreous humor at 980 in the temperature range of 24 to 40°C were measured. It was determined that any temperature dependence of the diffuse reflectance and total transmittance could not be discerned with the current setup in the temperature range of interest. The average  $R_d$  and  $T_t$  values over all measured temperatures were input into the inverse adding doubling (IAD) computer program yielding absorption and scattering coefficients of 0.75  $\text{cm}^{-1}$  and 0.03  $\text{cm}^{-1}$ , respectively. Values for absorption and scattering coefficient for bovine vitreous humor at room temperature reported by Sardar et al.<sup>2</sup> are 1.27  $\text{cm}^{-1}$  and 0.88  $\text{cm}^{-1}$ , respectively. Though the absorption coefficients are comparable the scattering coefficients are not. It is possible that some specular reflection was inadvertently measured in the work done by Sardar et al. No attempt was made to measure temperature dependent absorption and scattering coefficients at any other wavelengths for any sample.

The rate of change of the refractive index with respect to temperature,  $\frac{\partial n}{\partial T}$ , was performed at 632.8 nm for bovine aqueous and vitreous humor in the temperature range of 37 to 41°C using a Mach-Zehnder interferometer setup. The system was calibrated for water using data published by Schiebener et al.<sup>3</sup> The measured  $\frac{\partial n}{\partial T}(T)$  for bovine aqueous humor and vitreous humor were of the same order of magnitude of water. The measured  $\frac{\partial n}{\partial T}(T)$  of bovine aqueous humor was comparable to that of water, while the measured  $\frac{\partial n}{\partial T}(T)$  for bovine vitreous humor was slightly less. *These values, as yet not reported in literature, are necessary for accurately modeling thermal lensing and hence light propagation in the eye.*

## References

1. Prahl, S.A., Van Gemert, J.C., and Welch, A.J., "Determining the optical properties of turbid media by using the inverse adding-doubling method," *Appl. Opt.* **32** 559-568 (1993).
2. Sardar, D.K., Yin, G.Y., Yow, R.M., Thomas, R.J., and Tsin, A.T.C. "Optical properties of ocular tissues in the near infrared region", *Lasers Med. Sci.* (in press).
3. Schiebener, P., Straub, J., Sengers, J.M.H., and Gallagher J.S., "Refractive index of water and steam as function of wavelength, temperature and density", *J. Phys. Chem. Ref. Data* **19**(3) 677-717 (1990).
4. Yin, D.C., Inatomi, N.I., Wakayama, and Huang, W.D., "Measurement of temperature and concentration dependences of refractive index of hen-egg-white lysozyme solution", *Cryst. Res. Technol.* **38**(9) 785-792 (2003).

The following accomplishments were attained through support from the current grant:

### **Publications**

1. Sardar, D. K., Yow, R.M., Swanland, G.Y., Tsin, A.T., and Thomas, R.T., "Optical Characterization of Human Ocular Tissues in the Near Infrared Region," *Proceedings of SPIE – The International Society of Optical Engineering, Progress in Biomedical Optics and Imaging*, **6138** 613815 (2006).
2. Sardar, D.K, Yin, G.Y., Yow, R.M, Thomas, R.J., and Tsin, A.T. "Optical properties of ocular tissues in the near infrared region", *Lasers Med. Sci.* (in press).
3. Sardar, D.K., Yow, R.M, Schneider, E., Thomas, R.J., and Tsin, A.T.C. "Measurement of temperature dependence of refractive index of bovine ocular tissue", *J. Biomed. Opt.* (in preparation).

### **Presentations**

1. G.Y. Swanland, R.M. Yow, and D.K. Sardar, "Optical Properties of Bovine Ocular Tissues in the NIR" The Joint Fall Meeting of The Texas Section of AAPT, APS, and SPS, Houston, Texas, October 7-9, 2005.
2. D.K. Sardar, R.M.Yow, and A.T. Tsin, "Near Infrared Characterization of Optical Properties of Human Ocular Tissues" The SPIE International Symposium BiOS 2006, Biomedical Optics, San Jose, California, January 24-29, 2006.
3. T.T. Jobe, R.M. Yow, D.K. Sardar, and R.J. Thomas, "Finite-Difference Beam Propagation Modeling for Lasers in Ocular Tissues" The Texas Sections of the APS/AAPT/SPS Joint Spring Meeting, San Angelo, Texas, March 23-25, 2006.
4. G.Y. Swanland, R.M. Yow, D.K. Sardar, A.T. Tsin, and R.J. Thomas, "Optical Properties of Bovine Ocular Tissues in the Near Infrared Region" The Texas Section of the APS/AAPT/SPS Joint Spring Meeting, San Angelo, Texas, March 23-25, 2006.